Application of a Nitrospiropyran-FAD-Reconstituted Glucose Oxidase and Charged Electron Mediators as Optobioelectronic Assemblies for the Amperometric Transduction of Recorded Optical Signals: Control of the "On"−"Off" Direction of the Photoswitch

Ron Blonder,[†] Eugenii Katz,[†] Itamar Willner,*[,†] Victor Wray,[‡] and Andreas F. Bückmann[‡]

Contribution from the Institute of Chemistry and Farkas Center for Light-Induced Processes, The Hebrew University of Jerusalem, Jerusalem, 91904, Israel, and Gesellschaft für Biotechnologische Forschung, Department of Enzymology, Mascheroder Weg 1, D-38124 Braunschweig, Germany

Received August 4, 1997[⊗]

Abstract: Apo-glucose oxidase is reconstituted with the semisynthetic nitrospiropyran-FAD cofactor to yield a photoisomerizable glucose oxidase, **3a**-GOx. The nitrospiropyran-FAD-reconstituted GOx, **3a**-GOx, undergoes reversible photoisomerization to the protonated nitromerocyanine-FAD GOx, **3b**-GOx. The photoisomerizable enzyme was assembled as a monolayer on a Au electrode. The bioelectrocatalyzed oxidation of glucose in the presence of ferrocenecarboxylic acid (**4**), ferrocene-1,1′-dicarboxylic acid (**5**), or 1-[1-(dimethylamino)ethyl]ferrocene (**6**), acting as electron mediators, was examined in the different photoisomer states of the enzyme. With **4** and **5** acting as electron mediators, the enzyme in state **3b**-GOx exhibited bioelectrocatalytic activities for the oxidation of glucose. The bioelectrocatalytic functions of the enzyme in state **3a**-GOx were blocked in the presence of **4** or **5**. With **6** acting as electron mediator, the enzyme in state **3a**-GOx exhibits bioelectrocatalytic activities for the oxidation of glucose, whereas the bioelectrocatalytic functions of the **3b**-GOx state are blocked. The directionality of the enzyme photoswitch is controlled by the affinities of the oxidized electron mediators to diffusionally penetrate the protein and reach appropriate electron transfer distances to oxidize the $FADH_2$ redox center of the enzyme. In all of the systems, cyclic amperometric transduction of optical signals recorded by the photoisomerizable enzyme is accomplished. The enzyme photoisomer "on" or "off" switching direction is controlled by tuning the electrical interactions of the electron mediator and the photoisomerizable enzyme.

Photostimulated biomaterials provide the basis for the development of optobioelectronic devices.[1−3] The photochemical "on−off" control of the functions of biomaterials represents the optical recording event. The transduction of the recorded optical signal in the form of a secondary physical or electronic signal, represents the complementary function for the integrated operation of an optobioelectronic device. Amperometric transduction of optical signals was recently accomplished by photostimulation of redox proteins.[4] One method to photostimulate redox proteins involves the coupling of redox proteins (or redox enzymes) with photoisomerizable monolayer-modified electrodes. The photoisomerizable monolayer acts as a command interface that controls by light the protein and monolayer associative/dissociative interactions, and results in the photostimulated control of the protein electrical communication with the electrode surface. Light-controlled electrostatic interactions of cytochrome *c* or glucose oxidase with nitrospiropyran-modified Au electrodes led to the photostimulated amperometric transduction of optical signals recorded by the monolayer.[5,6] Another method to photostimulate redox enzyme involves the application of photoisomerizable diffusional electron mediators. In one photoisomer state of the electron relay mediation of the electron transfer between the enzyme redox center and the electrode occurs, and the biocatalyst is electrically activated for its characteristic biotransformation. In the complementary photoisomer state of the electron relay, the mediated electrical contact between the enzyme and the electrode is perturbed, and the bioelectrocatalytic activity of the enzyme is blocked. Nitrospiropyran-ferrocene and nitrospiropyran-*N*,*N*′-bipyridinium photoisomerizable electron relays were used to reversibly activate or inhibit the electrobiocatalytic activities of glucose oxidase and glutathione reductase, respectively.[7]

A further means to photostimulate redox enzymes includes the chemical modification of proteins with photoisomerizable components.[3,8,9] In one photoisomer state the tertiary protein structure is retained and it is in an active configuration for its biological function. In the complementary photoisomer state, the protein structure is distorted and its biocatalytic functions

* To whom correspondence should be addressed. Telephone: 972-2-6585272. Fax: 972-2-6527715. E-mail: willnea@vms.huji.ac.il .

[†] The Hebrew University of Jerusalem.

[‡] Gesellschaft für Biotechnologische Forschung.

[⊗] Abstract published in *Advance ACS Abstracts,* November 15, 1997.

(1) Willner, I.; Willner, B. In *Bioorganic Photochemistry*; Morrison, H., Ed.; Wiley: New York, **1993**; Vol. 2, pp 1−110.

(2) Willner, I.; Rubin, S. *Angew. Chem., Int. Ed. Engl.* **1996**, *35*, 367.

(3) Willner, I.; Rubin, S.; Riklin, A. *J. Am. Chem. Soc.* **1991**, *113*, 3321.

(4) Willner, I.; Lion-Dagan, M.; Marx-Tibbon, S.; Katz, E. *J. Am. Chem. Soc.* **1995**, *117*, 6581.

(5) Lion-Dagan, M.; Katz, E.; Willner, I. *J. Chem. Soc., Chem. Commun.* **1994**, 2741.

(6) Willner, I.; Doron, A.; Katz, E.; Levi, S.; Frank, A. J. *Langmuir* **1996**, *12*, 946.

(7) Lion-Dagan, M.; Marx-Tibbon, S.; Katz, E.; Willner, I. *Angew. Chem., Int. Ed. Engl.* **1995**, *34*, 1604.

(8) Willner, I.; Rubin, S.; Zor, T. *J. Am. Chem. Soc.* **1991**, *113*, 4013.

(9) Willner, I.; Lion-Dagan, M.; Rubin, S.; Wonner, J.; Effenberger, F.; Bäurele, P. *Photochem. Photobiol.* **1994**, *59*, 491.

S0002-7863(97)02663-2 CCC: $14.00

Scheme 1. Synthesis of Photoisomerizable-FAD Cofactor.

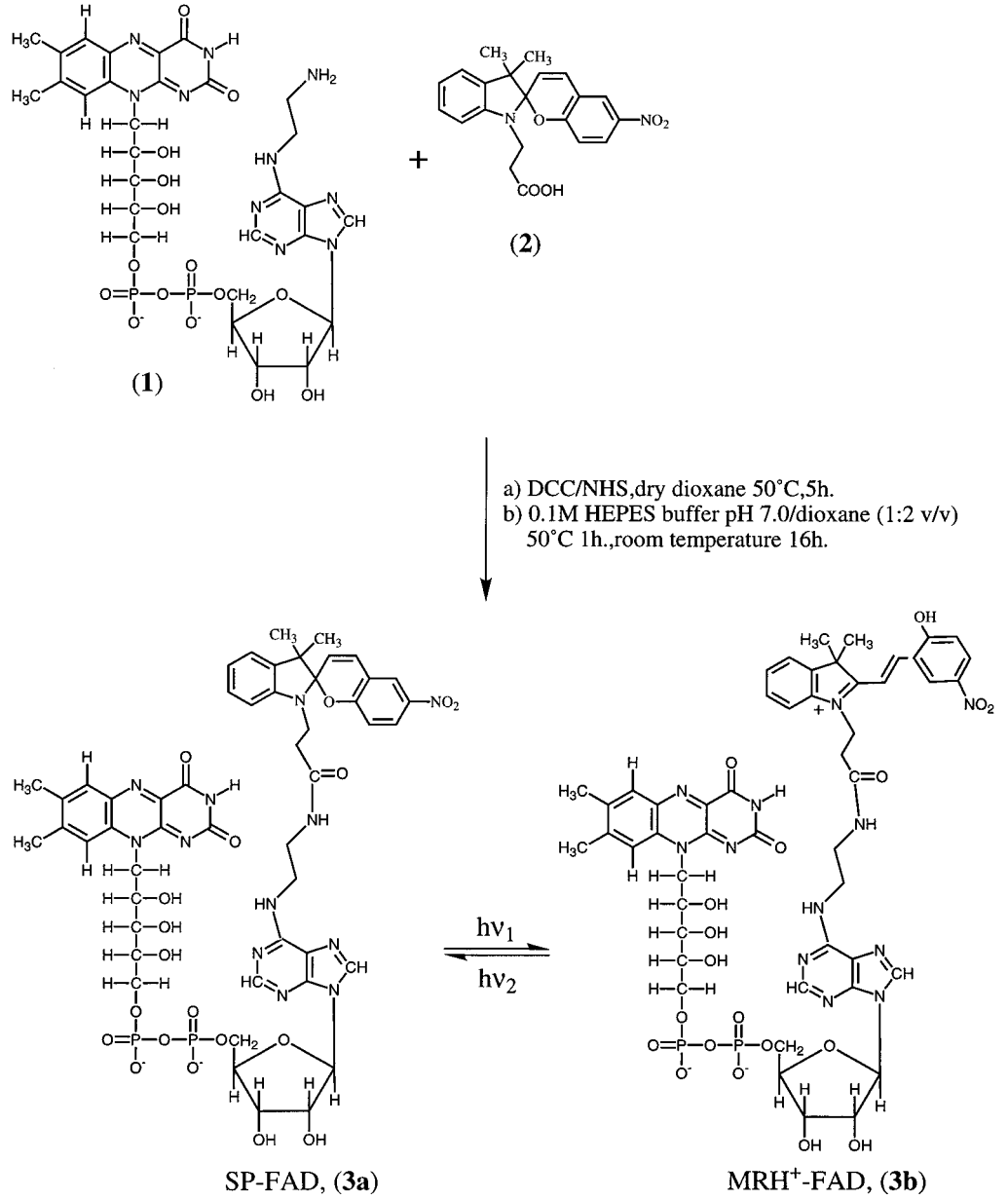

are blocked. By reversible photoisomerization of the light-active units, cyclic active and inactive forms of enzymes are generated. For example, photostimulation of glucose oxidase modified by nitrospiropyran photoisomerizable units enabled the cyclic amperometric transduction of optical signals recorded by the enzyme.[10] This method to photostimulate biomaterials suffers, however, from several limitations: (i) The loading degree affects the biocatalytic activities of the enzymes. At high loadings, substantial deactivation of the enzyme is observed. At lower loading degrees, the structural perturbations of the proteins are moderate, and, as a result, incomplete switched-off states are observed. (ii) Covalent modification of the protein is random, and the resulting enzyme represents a mixture of structurally modified proteins. This eliminates the possibility to correlate between microscopic structural perturbations of the protein, as a result of photoisomerization, and the bulk photoswitchable features of the biomaterial. (iii) Chemical modification of the redox proteins by photoisomerizable units does not allow us to predict light-induced switchable properties of the photoisomerizable proteins. That is, it is impossible to predict in what photoisomer state the protein structure is distorted. Thus, at present, it is impossible to predesign an enzyme photoisomer state that exhibits programmed "on" or "off" functions.

Recently, we reported on the design of new flavoenzyme properties by the reconstitution of the respective apoprotein with a semisynthetic flavin-adenine dinucleotide, FAD, cofactor.[11,12] It was demonstrated that reconstitution of apo-glucose oxidase with a ferrocene-modified FAD cofactor, results in a biocatalyst that electrically communicates with electrode surfaces.[12] Here we report on a novel method to photostimulate redox flavoenzymes by their reconstitution with a photoisomerizable semisynthetic FAD cofactor. The reconstitution of apo-glucose oxidase with nitrospiropyran FAD is described. The reconstitution method generates a site-specific modification of the protein with the photoisomerizable unit. The resulting photoisomerizable flavoenzyme exhibits complete "on−off" photostimulated

(10) Lion-Dagan, M.; Katz, E.; Willner, I. *J. Am. Chem. Soc.* **1994**, *116*, 7913.

(11) Willner, I.; Blonder, R.; Katz, E.; Stocker, A.; Bückmann, A. F. *J. Am. Chem. Soc.* **1996**, *118*, 5310.

(12) Riklin, A.; Katz, E.; Willner, I.; Stocker, A.; Bückmann, A. F. *Nature* **1995**, *376*, 672.

properties. We demonstrate a means to predesign the "on" or "off" states of the reconstituted enzyme by the integration of the photoactive enzyme electrode with appropriate electron mediators. We also reveal that the direction of the optically stimulated activation of a redox enzyme can be switched by the electrical charge associated with the electron mediator.

Experimental Section

Absorption spectra were recorded on a Uvikon-860 (Kontron) spectrophotometer. ^{1}H NMR spectra were recorded with a Bruker WM-400 (400.1 and 100.6 MHz), ^{13}C NMR spectra were recorded on a Bruker AM-300 (300.1 and 75.5 MHz). Negative ion electrospray ionization (ESI)-MS spectra were recorded on a Finnigan TSQ 700 instrument. Electrochemical measurements were performed using an electroanalyzer (EG&G, Versastat) linked to a personal computer (EG&G Research Electrochemistry Software Model 270/250). All electrochemical measurements were carried out in a three-compartment thermostated electrochemical cell consisting of a Au electrode (bare or modified) as a working electrode, a glassy carbon auxiliary electrode isolated by a glass frit, and a saturated calomel electrode (SCE) connected to the working volume by a Luggin capillary which was used as a reference electrode. All potentials are reported with respect to the SCE reference electrode. The electrochemical experiments were performed in a deaerated atmosphere and Ar was bubbled through the electrolyte prior to each measurement. When the electrolyte contains a protein, the deaerated atmosphere was generated by passing an Ar flow only above the electrolyte solution in order to prevent foams.

Glucose oxidase (from *Aspergillus niger*, GOx, EC 1.1.3.4) and all other chemicals, unless otherwise stated, were of commercial source (Merck, Aldrich, or Sigma). Ultrapure water from a nanopure (Bransted) source was used in all experiments. N^6-(2-aminoethyl)-FAD (**1**) was synthesized and characterized as previously described.[13] The nitrospiropyran 1-(β-carboxyethyl)-3,3-dimethyl-6′-nitrospiro[2*H*-1-benzopyran-2,1′-indoline] (**2**) was prepared according to the literature.[14] The nitrospiropyran-modified FAD, SP-FAD (**3**), was prepared by the coupling of **1** to **2** as outlined in Scheme 1. To a solution of **2** (0.038 g, 0.1 mmol) in 2 mL of dry dioxane was added dicyclohexylcarbodiimide (0.031 mg, 0.15 mmol), and *N*-hydroxysuccinimide (0.174 mg, 0.15 mmol) in 1 mL of HEPES buffer (0.1 M, pH 7.5) was added to the solution. After incubation of the clear solution at 50 °C for 4 h, a solution of **1** (0.08 g, 0.091 mmol) in 1 mL HEPES buffer (0.1 M, pH 7.5) was added. After the pH was adjusted to 7.0 with HCl (0.1 M), the turbid solution was stirred at 50 °C for 1 h and stirred further at room temperature for 16 h. After the reaction mixture was diluted with water to 25 mL and the pH adjusted to 4.5 with HCl (1 M), the solution was applied to a LiChroprep RP-18 reversed-phase column (Lobar, 310-25, 40−63 μM, Merck), integrated into a fast protein liquid chromatography (FPLC) system (Pharmacia) and equilibrated against water (pH 3.7, adjusted with HCl (0.1 M)) at room temperature. After gradient elution at room temperature [4000 mL, 0−60% methanol (v/v) in water 9 pH 3.7); 7 mL/min], concentration to 30 mL by rotation evaporation and lyophilization of the pooled fractions with pure product (**3**) (controlled by TLC[15], R_f: 0.4), 24.6 mg (**3**) was obtained in 23% yield (calculated for $C_{50}H_{56}O_{19}N_{12}P_2$ 1190; found ESI-MS [M − H] 1189). The ^{1}H and ^{13}C NMR assignments for **3** are summarized in Table 1 and 2, respectively.

Apo-GOx was prepared by a modification of the reported method.[16] GOx (200 mg) was dissolved in 0.025 M sodium phosphate buffer, pH = 6.0 (3 mL) that included glycerol (30% w/v). The solution was cooled to 0 °C and acidified to pH = 1.7 with a solution of 0.025 sodium phosphate−H_2SO_4, pH 1.1, that included glycerol 30%. The resulting solution was loaded on a Sephadex G-25 column (1.6 × 22 cm). The protein was eluted with 0.1 M sodium phosphate solution, pH 1.7, that included glycerol 30%. The eluted fractions were spectrophotometrically analyzed (λ = 280 nm), and the samples containing the protein were combined. To the protein solution was added Dextran-coated charcoal. The pH of the charcoal mixture was adjusted to pH 7.0 with 1 M NaOH and the solution was stirred for 1 h at 4 °C. The resulting solution was centrifuged (3400 rpm for 5 min) and filtered through a 0.45 μm filter. The resulting solution was dialyzed against a 0.1 M sodium phosphate buffer solution, pH = 7.0.

Reconstitution of apo-GOx with **3** was accomplished by mixing **3** (6×10^{-4} mmol) with apo-GOx (5.2×10^{-5} mmole) in 3 mL of 0.1 M sodium phosphate buffer, pH = 7.0. The solution was stirred at 30 °C for 4 h and then for an additional 12 h at 4 °C. The resulting mixture was dialyzed against 0.1 M sodium phosphate buffer, pH = 7.0, for 24 h.

Electrochemical transduction of the photoswitchable SP-FAD-reconstituted glucose oxidase electrobiocatalytic features in the presence of ferrocenecarboxylic acid (**4**), ferrocenedicarboxylic acid (**5**), and 1-[1-(dimethylamino)ethyl]ferrocene, (**6**), was examined using a bare Au-

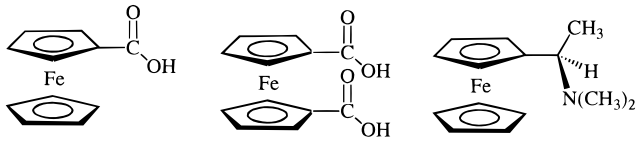

(**4**) (**5**) (**6**)

electrode and the biocatalyst, 0.46 mg mL^{-1}, the respective electron mediator at the corresponding concentration, and glucose 50 mM in the electrolyte solution, 2.5 mL. Prior to the electrochemical experiments, the protein content was determined by the Lowry method and the activity of the reconstituted enzyme was assayed using oxygen as electron acceptor for the oxidation of glucose. The generated H_2O_2 was spectrophotometrically analyzed by peroxidase and *o*-dianizidine. These assays were performed to ensure identical concentrations of the reconstituted enzyme in the different electrochemical systems.

SP-FAD-reconstituted glucose oxidase was assembled on a rough Au electrode in a monolayer configuration.[17] Au electrodes were roughened using mercury amalgam as reported previously.[18] Au electrodes were cleaned by treatment with a boiling 2 M solution of KOH for 1 h, rinsed with water and stored in concentrated sulfuric acid. The **3a**-GOx was assembled as a monolayer on a rough Au electrode. A cystamine (10 mM, 2 h) monolayer was assembled on a Au electrode. This was reacted with glutardialdehyde (5% in ethanol), and the resulting monolayer was reacted with **3a**-GOx to yield the biocatalyst monolayer.

Results and Discussion

N^6-(2-Aminoethyl)-FAD (**1**) was reacted with 1′-(β-carboxyethyl)-3′,3′-dimethyl-6′-nitrospiro[2*H*-1-benzopyran-2,1′-indoline] (**2**) to yield the FAD-nitrospiropyran, SP-FAD, derivative **3a** (Scheme 1). The SP-FAD (**3a**) exhibits reversible photoisomerizable properties. Upon irradiation of **3a**, 360 nm < λ < 380 nm, in an aqueous solution, protonated nitromerocyanine-functionalized FAD, MRH$^+$-FAD (**3b**), is formed. Further irradiation of **3b**, λ > 475 nm, restores the isomer **3a**. Figure 1 shows the absorption spectra of the SP-FAD and FAD-MRH$^+$.

The cyclic voltammogram of SP-FAD (**3a**) is shown in Figure 2. At pH 7, a reversible redox wave characteristic of the FAD unit at $E^\circ = -0.5$ V is observed. The redox potentials of the FAD component in the two photoisomers **3a** or **3b** are identical. Thus, the photoisomerizable unit does not affect the redox properties of the FAD site.

The semisynthetic photoswitchable glucose oxidase, GOx, was prepared by reconstitution of apo-GOx as outlined sche-

(13) Bückmann, A. F.; Wray, V.; Stocker, A. In *Methods in Enzymology: Vitamins and Coenzymes*; McCormick, D. B., Ed.; Academic Press: Orlando, 1997; Part I, Vol. 280, p 360.

(14) Namba, K.; Suzuki, S. *Bull. Chem. Soc. Jpn.* **1975**, *48*, 1323.

(15) Thin-layer chromatography is carried out on silica gel 60-F_{254} plates (0.2 mm; Merck) with a fluorescence marker in isobutyric acid/25% aqueous NH_3/H_2O (66:33:1, v/v/v), pH 3.7.

(16) Morris, D. L.; Buckler, R. T. In *Methods in Enzymology*; Langone, J. J., Van Vunakis, H., Eds.; Academic Press, Inc.: New York, **1983**, Part E, Vol. 92, pp 413−417.

(17) Riklin, A.; Willner, I. *Anal. Chem.* **1995**, *67*, 4118.

(18) Katz, E.; Schlereth, D. D.; Schmidt, H.-L. *J. Electroanal. Chem.* **1994**, *367*, 59.

Table 1. ^{1}H NMR Data for SP-FAD and Related Reference Compounds in DMSO-d_6 Containing a Trace of CD_3OD[a]

hydrogen	FAD	SP	SP-FAD[b]
		Adenosine Moiety	
A-2	8.12 (s)		8.20 (s)
A-8	8.46 (s)		8.38 (s)
A-11			3.22 (m)
A-12			3.47 (m)
A-1′	5.92 (d, 5.3)		5.93 (d, 4.8)
A-2′	4.54 (dd, 4.9, 4.9)		4.58 (dd)
A-3′	4.30 (m)		4.24 (m)
A-4′	4.07 (m)		4.08 (m)
A-5′	4.00 (m)		4.05 (m)[d]
		FAD Moiety	
F-6	7.81 (s)		7.86 (s)
F-9	7.92 (s)		7.93 (s)
F-7Me	2.35 (s)		2.37 (s)
F-8Me	2.42 (s)		2.44 (s)
F-1′A	4.99 (m)		5.00 (m)
F-1′B	4.60 (m)		4.61 (m)
F-2′	4.29 (m)		4.27 (m)
F-3′	3.72 (m)		3.70 (m)
F-4′	3.77 (m)		3.78 (m)
F-5′	4.00 (m)		4.05 (m)[d]
		Spiropyran Moiety	
S-4		7.12 (d, 7.4)	7.08 (d)
S-5		6.80 (dd, 7.4, 7.4)	6.77 (dd, 7.5, 7.5)
S-6		7.13 (dd, 7.4, 8.0)	7.10 (ddd, 7.7, 7.7, 1.1)
S-7		6.66 (d, 8.0)	6.64 (d, 7.8)
S-3′		5.99 (d, 10.4)	5.95 (d, 10.4)
S-4′		7.20 (d, 10.4)	7.17 (d, 10.4)
S-5′		8.21 (d, 2.8)	8.19 (d, 2.7)
S-7′		8.00 (dd, 9.0, 2.9)	*c*
S-8′		6.86 (d, 9.0)	6.84 (d, 9.0)
S-9A		3.49 (ddd, 14.9, 8.1, 6.9)	3.47 (m)
S-9B		3.38 (ddd, 14.8, 7.8, 6.0)	3.34 (m)
S-10A		2.57 (ddd, 15.8, 7.5, 6.5)	2.42 (m)
S-10B		2.45 (ddd, 15.9, 8.3, 5.9)	2.13 (m)
S-12		1.08 (s)	1.04 (s)
S-13		1.19 (s)	1.16 (s)

[a] Key: A, adenine moiety; F, FAD moiety; S nitrospiropyran moiety [b] The signals in the adenosine and FAD moieties are poorly resolved and the assignments follow from the COSY connectivities. [c] This is split into two signals of equal intensity and is the only signal in the spectrum that shows an unambiguous doubling under these solution conditions. Data are as follows: 7.98 (dd, 8.9, 2.3); 7.97 (dd, 9.0, 2.6). [d] The shift was taken from the correlation in the one-bond $^{13}C-^1H$ correlation.

matically in Figure 3. The native FAD cofactor was excluded from GOx to yield apo-GOx. The apoprotein was interacted with the semisynthetic photoisomerizable FAD cofactor **3a** to generate **3a**-GOx. The resulting reconstituted protein exhibits reversible photoisomerizable properties. Irradiation of **3a**-GOx, 360 nm $< \lambda <$ 380 nm, yields **3b**-GOx. Further illumination of **3b**-GOx with visible light $\lambda >$ 475 nm, restores **3a**-GOx. The absorption spectrum of **3a**-GOx exhibits the characteristic FAD absorbance band, $\lambda = 453$ nm. From the FAD absorbance ($\epsilon = 14\,000$ M^{-1} cm^{-1}), of a protein sample of known concentration, the loading of **3a** in the reconstituted protein is calculated to correspond to 2. Native GOx consists of two subunits and each of these includes a FAD cofactor component. Thus, the semisynthetic photoisomerizable FAD cofactor **3a** is introduced into each of the subunits of the apoprotein. The activities of **3a**-GOx and **3b**-GOx were compared to that of native GOx by assaying the biocatalyzed oxidation of glucose by molecular oxygen by the different biocatalysts, and analysis of the generated H_2O_2 in the various systems, with peroxidase and *o*-dianisidine used as a colorimetric probe. We find that MRH^+-GOx, **3a**-GOx, retains 80% of the biocatalytic activity of native GOx. Comparison of the biocatalyzed activities of **3a**-GOx and **3b**-GOx reveals that **3b**-GOx is ~10% more active than **3a**-GOx. Thus, with oxygen as electron acceptor, the two photoisomer states of the reconstituted protein exhibit high biocatalytic properties. Although the difference in activities of the photoisomer states **3a**-GOx and **3b**-GOx is small, the results are very reproducible, suggesting that oxidation of the FAD sites in **3a**-GOx by molecular oxygen is indeed inhibited. Thus the oxidation of the FAD units by the low molecular weight oxygen acceptor is not significantly affected by the photoisomerizable component, suggesting that the structural distortions induced by the photoisomerizable unit are not sufficient to perturb the electron transfer between O_2 and the cofactor units (*vide infra*). The results suggest, however, that the application of bulky electron acceptors that substitute O_2 could provide a means to amplify the difference in the biocatalytic properties of the photoisomer states of the SP-FAD-reconstituted GOx.

Synthetic electron-transfer relays, such as ferrocene derivatives,[19] quinones or ferricyanide, mediate electrical communication between the FAD sites of GOx and electrode supports.[20] These electron mediators substitute molecular oxygen as electron acceptor, and electrochemical regeneration of the charge mediator facilitates electrobiocatalyzed oxidation of glucose. The electrobiocatalyzed oxidation of glucose by **3a**-GOx and **3b**-GOx in the presence of ferrocenecarboxylic acid (**4**) as diffusional electron mediator was examined (Figure 4). Both photoisomer states of the biocatalyst reveal bioelectrocatalytic properties, as reflected by the electrocatalytic anodic currents

(19) Bartlett, P. N.; Tebbutt, P.; Whitaker, R. G. *Prog. React. Kinet.* **1991**, *16*, 55.

(20) Cass, A. E. G.; Davis, G.; Francis, G. D.; Hill, H. A. O.; Aston, W. J.; Higgins, I. J. Plotkin, E. V.; Scott, L. D. L.; Turner, A. P. F. *Anal. Chem.* **1984**, *56*, 667.

Table 2. ^{13}C NMR Data for SP-FAD and Related Reference Compounds in DMSO-d_6 Containing a Trace of CD_3OD[a]

carbon	FAD	SP	SP-FAD	method[b]
		Adenosine moiety		
A-2	152.8		*c*	
A-4	149.7		*c*	
A-5	118.8		*c*	
A-6	156.0		*c*	
A-8	139.6		*c*	
A-11			38.1	D
A-12			39.5	D
A-1′	87.1		86.8	D
A-2′	74.3		73.5	D
A-3′	70.4		70.3	D
A-4′	83.8[f]		83.2	D
A-5′	64.5[f]		64.6	D
		FAD Moiety		
F-2	156.0		*d*	
F-4	160.1		*d*	
F-6	130.8		130.4	D/L
F-7	136.0		135.7	L
F-8	146.5		146.1	L
F-9	117.7		117.4	D/L
F-11	132.2		132.0	L
F-12	134.2		134.0	L
F-13	136.7		*e*	
F-14	151.0		*d*	
F-7Me	l8.8		l8.6	D/L
F-8Me	20.8		20.6	D/L
F-1′	47.6		*e*	
F-2′	69.3		68.8	D
F-3′	72.6		72.1	D
F-4′	71.9[f]		71.3	D
F-5′	67.1[f]		66.9	D
		Spiropyran Moiety		
S-2		106.4	106.6	L
S-3		52.4	52.5	L
S-3a		135.6	135.7	L
S-4		121.7	121.3	D/L
S-5		119.2	119.0	D/L
S-6		127.6	127.3	D/L
S-7		106.6	106.5	D/L
S-7a		146.0	146.4	L
S-3′		122.7	122.9	L
S-4′		128.1	127.7	D
S-4′a		118.8	118.8	L
S-5′		121.7	122.5	D
S-6′		140.5	140.6	L
S-7′		125.6	125.1	D
S-8′		115.4	115.2	D
S-8′a		159.0	159.2	L
S-9		38.8	39.2	D
S-10		33.1	39.6	D/L
S-11		172.7	170.6	L
S-12		19.4	19.2	D/L
S-13		25.5	25.4	D/L

[a] Key: A, adenine moiety; F, FAD moiety; S, nitrospiropyran moiety. [b] The shifts were determined from the positions of the cross peaks in either the ^1H-detected one-bond (D) or multiple-bond (L) $^{13}C-^1H$ correlations and calibrated against the signal for the solvent at 39.5 ppm. [c] Not determined as the $^{13}C-^1H$ interactions of H-2 and H-8 were not detected. [d] Not accessible by either correlation. [e] Not determined as the $^{13}C-^1H$ interactions of H-1′AB were not detected. [f] Broadened through coupling to ^{31}P.

observed at the redox potential corresponding to **4**. The electrocatalytic anodic current is, however, enhanced in the presence of **3b**-GOx, indicating that the MRH^+-GOx photoisomer exhibits higher bioelectrocatalytic activity compared to that of **3a**-GOx, using **4** as electron mediator. The electrocatalytic anodic current is proportional to the rate of electrobiocatalyzed oxidation of glucose. Thus we analyzed the kinetic features of the two photoisomer states of the reconstituted enzyme, **3a**-GOx and **3b**-GOx, according to the Michaelis−Menten model. As the biocatalyzed oxidation of glucose involves two cosubstrates, glucose and ferrocenecarboxylic acid, eqs 1 and 2, the kinetic analyses for each of the cosubstrates,

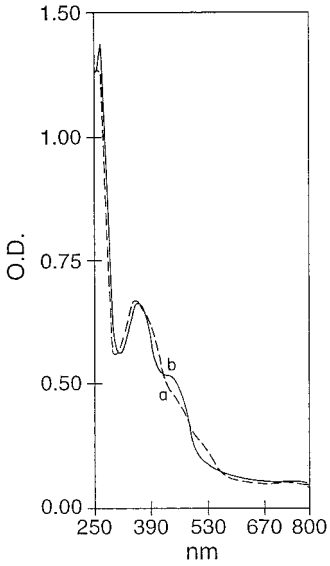

Figure 1. Absorption spectra of the photoisomerizable (**3**) in TDW: (a) MRH^+-FAD state formed by irradiation, 360 nm < λ < 380 nm; (b) SP-FAD state, generated by illumination, λ > 475 nm.

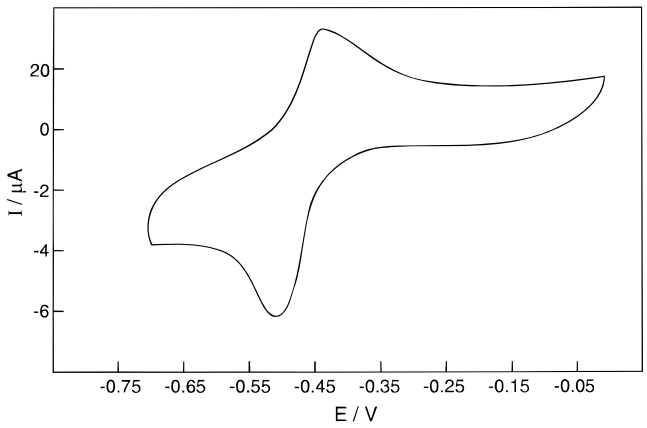

Figure 2. Cyclic voltammograms of a bare gold electrode in the presence of SP-FAD, 10^{-4} M, 0.1 M phosphate buffer, pH 7.0; scan rate was 200 mV s^{-1}.

$$GOx{-}FAD_{red} + Fc^+ \underset{k_-}{\overset{k_+}{\rightleftharpoons}} GOx{-}FAD_{red}\cdots Fc^+ \xrightarrow{k_{cat}} GOx{-}FAD_{ox} + Fc \quad (1)$$

$$GOx{-}FAD_{ox} + \text{glucose} \underset{k'_-}{\overset{k'_+}{\rightleftharpoons}} GOx{-}FAD_{ox}\cdots\text{glucose} \xrightarrow{k'_{cat}} GOx{-}FAD_{red} + \text{gluconic acid} \quad (2)$$

were performed under conditions where the complementary substrate is at saturation. Following this approach the rate-limiting conditions for the biocatalyzed transformations of each of the cosubstrates can be elucidated, and the specific photoswitchable activities of **3a**-GOx or **3b**-GOx toward each of the co-substrates can be determined. The electrocatalytic anodic currents were recorded at different concentrations of the two substrates. Figure 5A shows the anodic currents transduced by the **3a**-GOx and **3b**-GOx biocatalysts at different concentrations of **4**. Figure 5B shows the Lineweaver−Burk plots of these

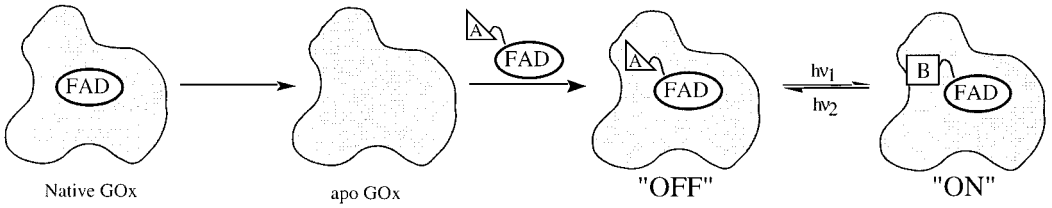

Figure 3. Design of a photoswitchable biocatalyst by reconstitution of a flavoenzyme by a semisynthetic photoisomerizable FAD cofactor.

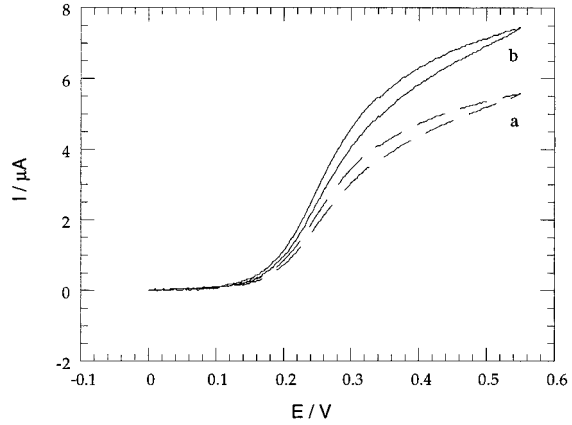

Figure 4. Cyclic voltammograms for the bioelectrocatalyzed oxidation of glucose, 5×10^{-2} M, and ferrocene carboxylic acid (**4**), 5×10^{-4} M, in the presence of (a) (SP-FAD)-GOx, 0.46 mg mL^{-1}, and (b) (MRH^+-FAD)-GOx, 0.46 mg mL^{-1}. All experiments were recorded in a phosphate buffer, 0.1 M, pH 7.0, 37 °C, under argon. Scan rate was 5 mV s^{-1}. Electrode surface area was 0.22 cm^2.

data according to eq 3, where K_m is given by eq 4. Figure 5C

$$\frac{1}{I} = \frac{K_m}{I_{max}[Fc^+]} + \frac{1}{I_{max}} \quad (3)$$

$$\frac{1}{I} = \frac{K_m}{I_{max}[\text{glucose}]} + \frac{1}{I_{max}} \quad (4)$$

shows the respective Lineweaver−Burk plots for **3a**-GOx and **3b**-GOx with glucose as substrate. The two photoisomer states exhibit similar K_m and I_{max} values for the glucose substrate. This suggests that the two photoisomer states of GOx reveal similar binding affinities for glucose and identical biocatalytic oxidation features for the glucose substrate. For the ferrocenecarboxylic acid cosubstrate **4**, the two photoisomer enzyme states, **3a**-GOx and **3b**-GOx, reveal similar I_{max} values, $I_{max} = 9.6\ \mu A$, but their K_m values differ substantially: $K_m = 0.8$ mM for **3a**-GOx and $K_m = 0.3$ mM for **3b**-GOx. The identitical I_{max} values for the two enzymes with respect to **4** suggests that the mediated electron transfer from the FAD unit to the electrogenerated ferrocenylium cation is of similar effectiveness in the two photoisomeric enzymes. The different K_m values of **4** for the two enzymes indicates, however, different affinities of the two proteins for the ferrocenylium cation electron mediator. As no specific binding site for the ferrocenylium cation exists in the proteins, the term "affinity" reflects the interactions of the electron transfer mediator and the protein along the penetration path to the appropriate distance that enables electrical communication with the FAD. For **3b**-GOx the penetration path is facilitated as reflected by the lower K_m value. Upon photoisomerization to **3a**-GOx, the protein is structurally distorted and the penetration path of the electron-transfer mediator is perturbed. This is reflected by the higher K_m value of the protein, and the resulting lower bioelectrocatalytic activity of the enzyme. The kinetic analysis of the biocatalytic properties

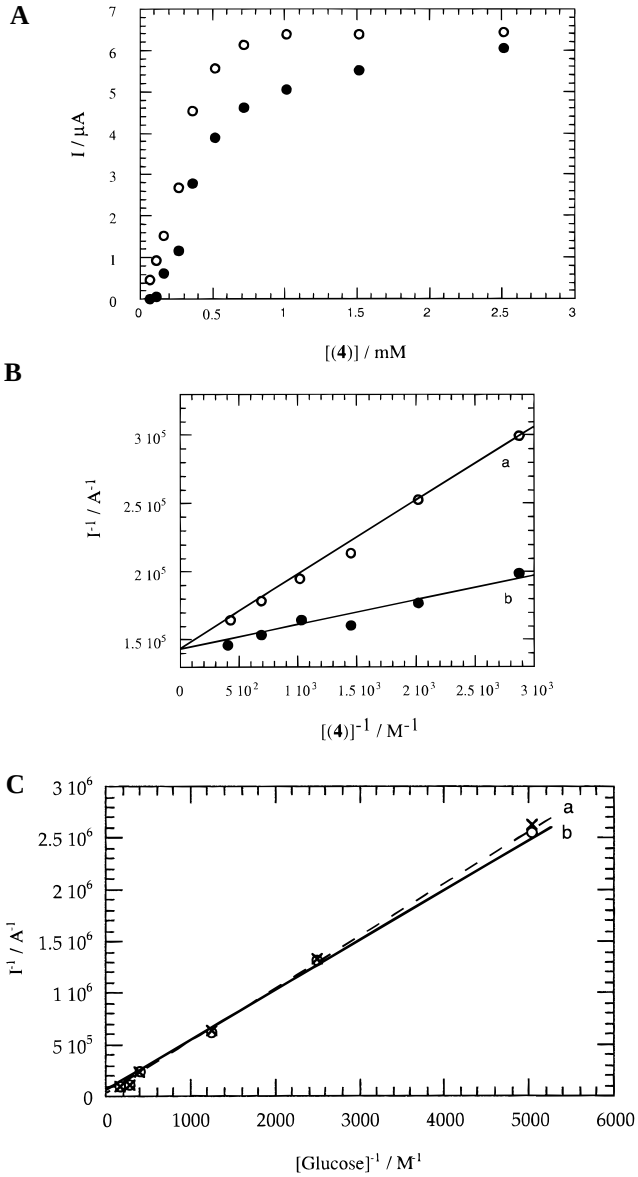

Figure 5. (A) Electrocatalytic anodic current developed by the photoisomerizable GOx at different concentrations of ferrocene carboxylic acid, (**4**): (●) with (SP-FAD)-GOx, 0.46 mg mL^{-1} and (○) with (MRH^+-FAD)-GOx, 0.46 mL^{-1}. All systems include glucose, 5×10^{-2} M, in phosphate buffer, 0.1 M, pH 7.0, under argon, 37 °C. (B) Linweaver−Burk plot for the saturation current curves shown in A: (a) for (SP-FAD)-GOx and (b) for (MRH^+-FAD)-GOx. (C) Linweaver−Burk plot for glucose: (a) for (SP-FAD)-GOx; (b) for (MRH^+-FAD)-GOx. All systems include **4**, 50 mM, in phosphate buffer, 0.1 M, pH 7.0, under argon, 37 °C.

of **3a**-GOx and **3b**-GOx allows us to select the appropriate concentration of the ferrocene carboxylic acid cosubstrate for maximal light-stimulated switchable activities of **3a**-GOx and **3b**-GOx.

The reconstituted photoisomerizable enzyme, (**3**)-GOx, was applied to organize an optobioelectronic device. The biocatalyst

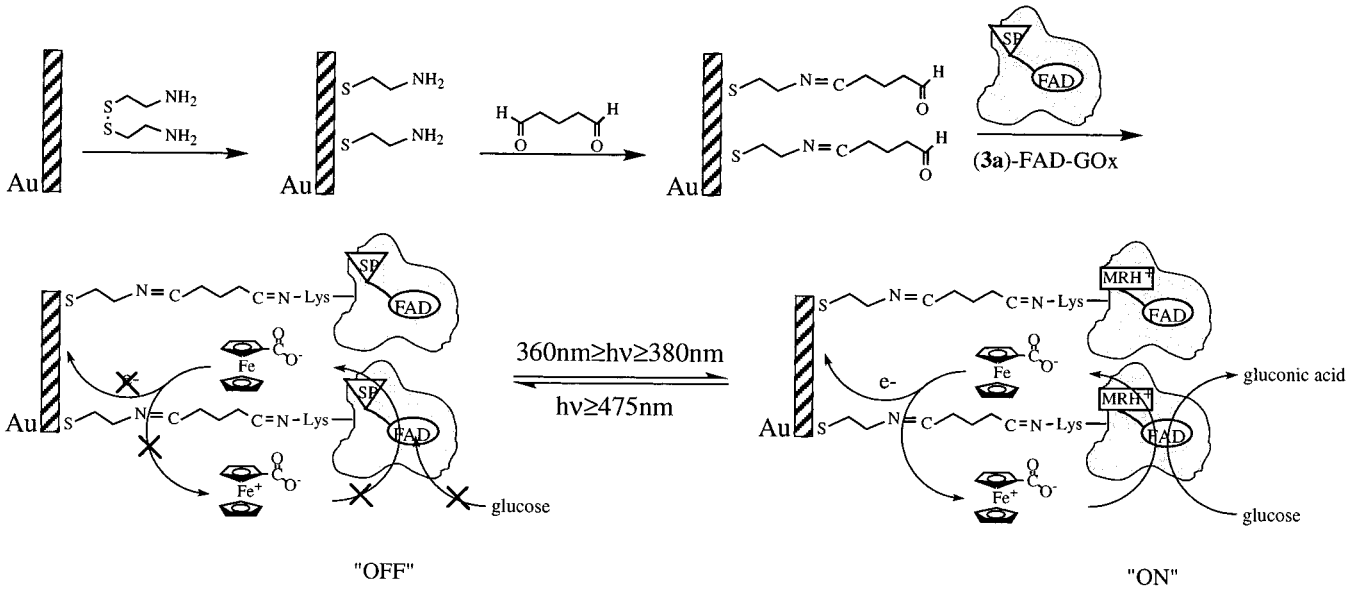

Figure 6. Organization of reconstituted photoisomerizable GOx as a monolayer on a Au electrode.

was assembled as a monolayer on a rough Au electrode as outlined in Figure 6. A cystamine monolayer was assembled on a Au electrode. This was reacted with glutardialdehyde to yield the carbonyl-functionalized Schiff base interface, and the resulting monolayer was reacted with **3a**-GOx to yield the biocatalyst monolayer. The cyclic voltammograms[21] of the photoisomerizable biocatalyst monolayer in the presence of ferrocene carboxylic acid, 5×10^{-5} M, as diffusional electron-transfer mediator and glucose, 5×10^{-2} M, are shown in Figure 7A. In the presence of **3b**-GOx monolayer, an electrocatalytic anodic current is observed, indicating the bioelectrocatalyzed oxidation of glucose (Figure 7A, curve a). Upon photoisomerization of the monolayer electrode to the **3a**-GOx state, $\lambda >$ 475 nm, the cyclic voltammogram shown in Figure 7A, curve b, is observed. This cyclic voltammogram almost overlaps the cyclic voltammogram of the enzyme-functionalized electrode in the absence of glucose and corresponds to the amperometric response of the electron mediator alone (Figure 7A, curve e). Thus, the **3a**-GOx monolayer electrode is not active in the bioelectrocatalyzed oxidation of glucose. Further isomerization of the **3a**-GOx monolayer electrode, 360 nm $< \lambda <$ 380 nm, to the **3b**-GOx monolayer restores the electrocatalytic anodic current. By cyclic photoisomerization of the enzyme monolayer between the **3b**-GOx and **3a**-GOx state, the reversible activation and deactivation of the electrobiocatalyzed oxidation of glucose is stimulated, respectively (Figure 7B). Thus, organization of the photoisomerizable enzyme as a monolayer on the electrode surface provides a means for the amperometric transduction of optical signals recorded by the monolayer. By selection of the appropriate concentration of the electron mediator, almost complete "on−off" photoswitchable activation and deactivation of the biocatalyst is accomplished.

Two other electron mediator substrates, ferrocene-1,1′-dicarboxylic acid (**5**) and 1-[1-(dimethylamino)ethyl]ferrocene (**6**) were used to electrically communicate the photoisomerizable enzymes, **3a**-GOx and **3b**-GOx, with the electrode. Note that the charge carrier for oxidation of the flavoenzyme is the electrogenerated ferrocenyl cation. At the pH used for bioelectrocatalyzed oxidation of glucose, pH 7, the carboxylic acid residues in **4** and **5** are deprotonated, whereas the amine function of **6** is in a protonated form. Thus, the overall charge of the electron mediator oxidizing the flavoenzyme is 0, −1, and +2 for **4**, **5**, and **6**, respectively. Figure 8A shows the electrocatalytic anodic currents resulting from the bioelectrocatalyzed oxidation of glucose by **3a**-GOx and **3b**-GOx in the presence of ferrocene-1,1′-dicarboxylic acid as electron mediator. **3b**-GOx reveals substantially enhanced anodic currents as compared to those developed by **3a**-GOx. The analysis of the electrocatalytic anodic currents developed by **3a**-GOx and **3b**-GOx at different concentrations of (**5**) according to the Lineweaver−Burk equation (eq 3), is shown in Figure 8B. The two enzyme states **3a**-GOx and **3b**-GOx exhibit a similar $I_{max} = 60\ \mu$A value but differ substantially in their K_m values: $K_m = 5.0\ \mu$M for **3b**-GOx and $K_m = 0.2$ mM for **3a**-GOx. The affinity of the **3b**-GOx for the electron transfer mediator, **5**, is substantially higher than that of **3a**-GOx. Comparison of the K_m values of **5** and **4** with respect to **3a**-GOx and **3b**-GOx reveals that while **4** and **5** reveal similar affinities to **3a**-GOx, **5** exhibits a substantially higher affinity than **4** for **3b**-GOx. That is, the penetration path of ferrocenyl-1,1′-dicarboxylate cation ($\mathbf{5}^+$) to the FAD site is facilitated. The enhanced affinity of oxidized **5** for **3b**-GOx results in a high electrocatalytic anodic current at low concentrations of **5**. Note that the I_{max} values of **3b**-GOx in the presence of **4** and **5** are almost identical, implying almost similar electron-transfer rates from the $FADH_2$ site to the respective oxidized electron mediators. The saturation currents are, however, observed with an ∼10-fold lower concentration of the electron mediator **5** as compared to the concentration of **4**. This suggests that the affinity of oxidized **5** is substantially higher than that of oxidized **4** for **3b**-GOx. The high affinity of **5** to **3b**-GOx results in enhanced electron-transfer turnover rates at the lower concentration of **5**. The electron-transfer mediator **5** was similarly applied for reversible amperometric transduction of optical signals recorded by the photoisomerizable enzyme−monolayer electrode. The electrocatalytic anodic currents developed by **3a**-GOx and **3b**-GOx states, 0.46 mg mL^{-1}, in the presence of **5**, were recorded (Figure 9A). In the presence of **3a**-GOx monolayer, no electrocatalytic anodic current is observed, indicating that the protein is switched-off for the electrobiocatalyzed oxidation of glucose. Photoisomerization of **3a**-GOx to the **3b**-GOx state, 360 nm $< \lambda <$ 380 nm, results in a high electrocatalytic anodic current reflecting the switched-on electrobiocatalyzed oxidation

(21) The cyclic voltammogram of the enzyme mopnolayer does not show the characteristic reversible wave of the isolated photoisomerizable FAD unit. This indicates that the FAD unit is embedded in the protein and lacks direct electrical communication with the electrode.

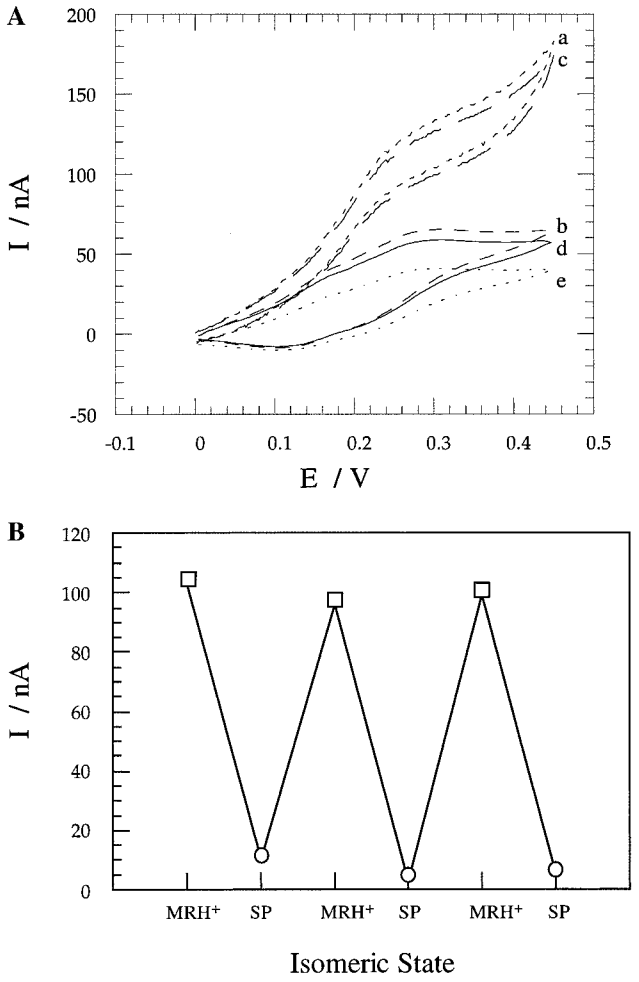

Figure 7. (A) Cyclic voltammograms of the photoisomerizable monolayer electrode in the presence of glucose, 50 mM, and **4**, 50 μM: (a and c) with the (MRH$^+$-FAD)-GOx electrode; (b and d) with the (SP-FAD)-GOx electrode; and (e) with the (SP-FAD)-GOx electrode and **5**, 50 μM, in the absence of glucose. All experiments were recorded in phosphate buffer, 0.01 M and pH 7.3, and sodium sulfate, 0.1 M, 37 °C, under argon. A Au foil electrode, geometrical area 0.4 cm^2 (roughness coefficient ~20) was used, scan rate, 5 mV s^{-1}. (B) Cyclic amperometric transduction of optical signals recorded by the reconstituted photoisomerizable GOx electrode. Net electrocatalytic anodic currents at $E = 0.4$ V are presented.

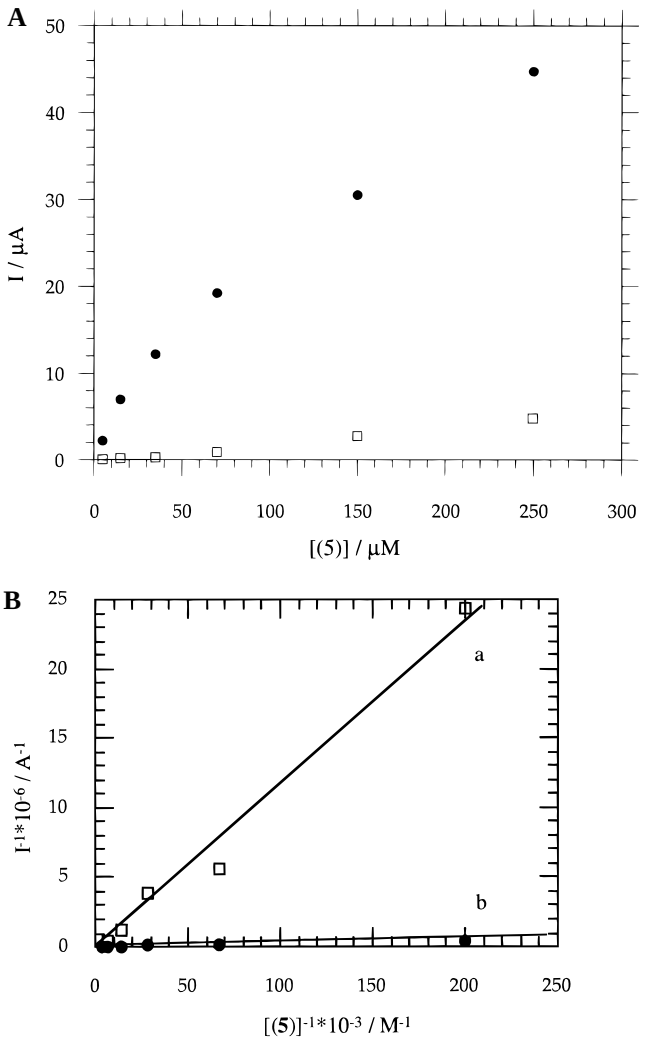

Figure 8. (A) Electrocatalytic anodic current developed by the photoisomerizable GOx at different concentrations of **5**: (□) with (SP-FAD)-GOx, 0.46 mg mL^{-1} and (●) with (MRH$^+$-FAD)-GOx, 0.46 mg mL^{-1}. All experiments include glucose, 50 mM, in phosphate buffer, 0.1 M, pH 7.0, under argon, 37 °C. (B) Lineweaver−Burk plot for the saturation current curves shown in A: (a) for (SP-FAD)-GOx and (b) for (MRH$^+$-FAD)-GOx.

of glucose. Further irradiation, $\lambda > 475$ nm, of the functionalized electrode regenerates the **3a**-GOx state and the biocatalyzed oxidation is switched to the "off" state. By cyclic isomerization of the enzyme between the **3a**-GOx and **3b**-GOx monolayer states, reversible "off" and "on" states of the biocatalyst are generated respectively (Figure 9B).

The most intriguing results are observed upon the application of 1-[1-(dimethylamino)ethyl]ferrocene (**6**) as electron-transfer mediator. Figure 10A shows the electrocatalytic anodic currents developed by **3a**-GOx and **3b**-GOx at different concentrations of **6**. In contrast to the previous systems, **3a**-GOx reveals enhanced electrocatalytic currents as compared to **3b**-GOx. Figure 10B shows the kinetic analysis of the anodic current at different concentrations of **6**, according to eq 3. As before, the two enzyme states **3a**-GOx and **3b**-GOx reveal similar I_{max} values, $I_{max} = 9$ μA. The two enzyme states differ, however, in their K_m values, $K_m = 0.5$ mM for **3a**-GOx and $K_m = 50$ mM for **3b**-GOx. This implies that the electrooxidized **6** exhibits a higher affinity for penetrating the biocatalyst in the state **3a**-GOx. Thus, we clearly observe a different direction of affinities of the photoisomerizable enzyme for the different ferrocene electron mediators. While **3b**-GOx exhibits high affinity for **4** and **5**, **3a**-GOx reveals an increased affinity for **6**.

The photoisomerizable enzyme was assembled as a monolayer on the Au electrode, and the resulting enzyme electrode was used to reversibly activate and deactivate the electrobiocatalyzed oxidation of glucose in the presence of **6** as electron-transfer mediator (Figure 11A). In the presence of **3a**-GOx, a high electrocatalytic anodic current is observed. Photoisomerization 360 nm $< \lambda <$ 380 nm of the enzyme to the **3b**-GOx state blocks the electrobiocatalyzed oxidation of glucose and only the background electroresponse of the electron mediator is observed. Further isomerization of the **3b**-GOx monolayer to the **3a**-GOx state restores the bioelectrocatalytic activity of the enzyme electrode. By reversible photoisomerization of the enzyme monolayer between the states **3a**-GOx and **3b**-GOx cyclic amperometric transduction of the recorded optical signal is accomplished (Figure 11B). Note that in contrast to the two previous systems, where **4** and **5** were employed as electron-transfer mediators and the enzyme state **3b**-GOx acted as the active biocatalyst transducing the amperometric signal, in the presence of **6** as electron carrier, the enzyme in the **3a**-GOx state is the active form for transduction of the amperometric signal. Thus, the electroactive optical switch direction of the

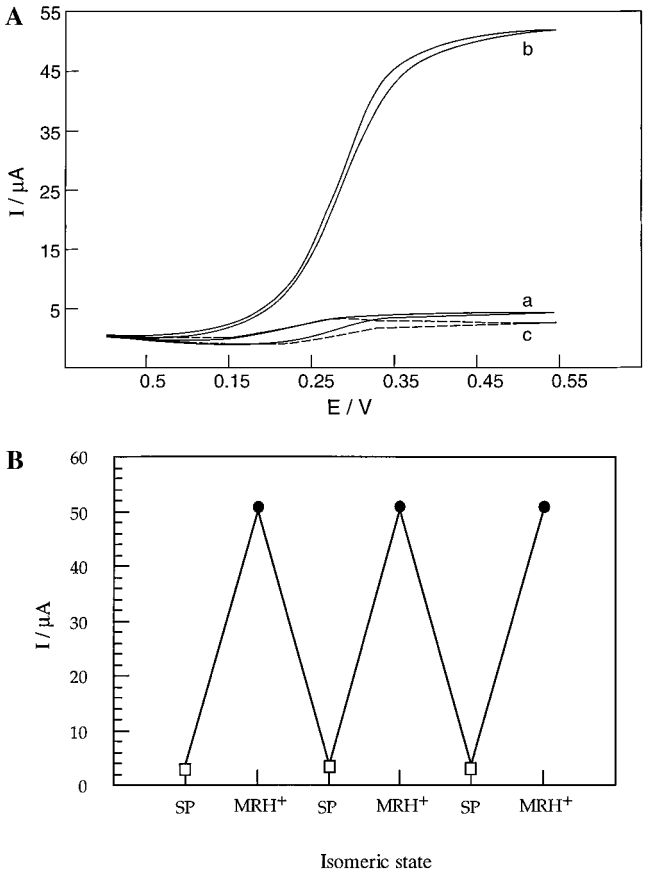

Figure 9. (A) Cyclic voltammograms for the bioelectrocatalyzed oxidation of glucose, 50 mM, and **5**, 0.25 mM, in the presence of (a) (SP-FAD)-GOx, 0.46 mg mL^{-1}; (b) (MRH^+-FAD)-GOx, 0.46 mg mL^{-1}; and (c) no enzyme. All experiments were recorded under the same conditions as described in Figure 4. (B) Cyclic amperometric transduction of optical signals recorded by the reconstituted photoisomerizable GOx, 0.46 mg μm L^{-1}, **5**, 25 μM, and glucose, 50 mM, in the electrolyte solution. Net electrocatalytic currents at $E = 0.4$ V are presented.

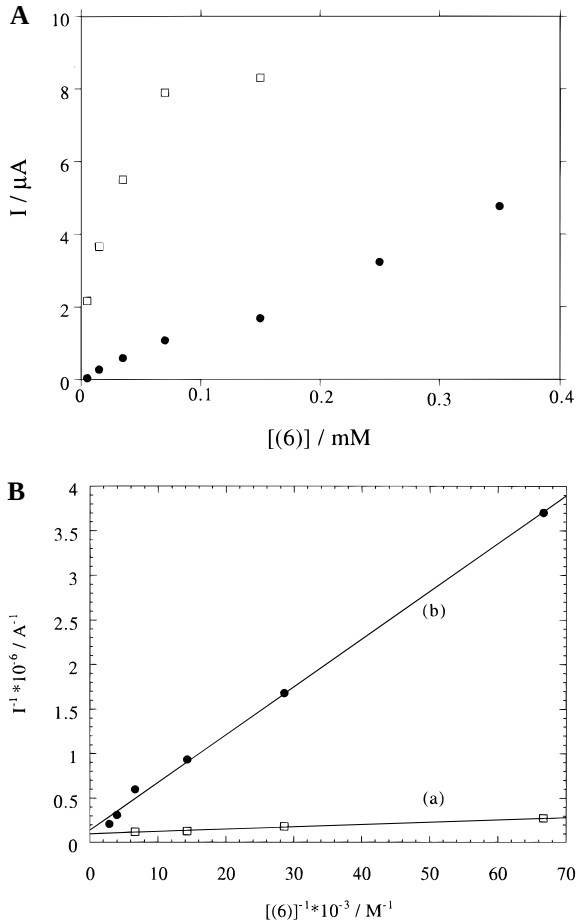

Figure 10. (A) Electrocatalytic anodic current developed by the photoisomerizable GOx at different concentrations of **6**: (□) With (SP-FAD)-GOx, 0.46 mg mL^{-1} and (●) With (MRH^+-FAD)-GOx, 0.46 mg mL^{-1}. All experiments include glucose, 50 mM, in phosphate buffer, 0.1 M, pH 7.0, under argon, 37 °C. (B) Lineweaver−Burk plot for the saturation current curves shown in A (a) for (SP-FAD)-GOx and (b) for (MRH^+-FAD)-GOx.

reconstituted photoisomerizable enzyme can be controlled by the nature of electron-transfer mediator. With ferrocenecarboxylic acid (**4**) and ferrocenedicarboxylic acid (**5**), the enzyme state **3b**-GOx represents the switched-on biocatalyst. In the presence of 1-[1-(dimethylamino)ethyl]ferrocene (**6**) the biocatalyst in the isomer state **3a**-GOx is switched-on for the bioelectrocatalyzed oxidation of glucose.

To account for the effects of the nature of electron-transfer mediator on the photoswitch direction of the reconstituted photoisomerizable glucose oxidase, we first compare the electron mediators **5** and **6**. Ferrocenedicarboxylic acid (**5**) at pH 7.0 is deprotonated to a ferrocene unit bearing two negative charges, where 1-[1-(dimethylamino)ethyl]ferrocene (**6**) at this pH value is protonated to the respective ammonium ion. Upon electrooxidation, **5** yields an electron-transfer mediator exhibiting a net negative charge (−1). Electrooxidation of **6** yields, in turn, a double positively charged electron transfer mediator, (+2) (Figure 12). The photoisomer unit linked to the FAD cofactor is neutral in the nitrospiropyran state **3a**-GOx. The nitromerocyanine isomer state, formed upon photoisomerization of **3a**-GOx, is protonated at pH = 7.0 and thus the photoisomer unit linked to the FAD cofactor is positively charged. As a result, penetration of oxidized **5** to the redox-active FAD site is assisted by electrostatic attractive interactions in the presence of **3b**-GOx. In turn, penetration of the positively charged oxidized **6** into the **3b**-GOx isomer state is perturbed due to electrostatic repulsion of the oxidized electron mediator from the FAD site by the protonated merocyanine photoisomer unit. Thus, the delicate control of the electrostatic interactions of the electron-transfer mediators with the photoisomerizable units, controls the photochemical switch direction of the reconstituted biocatalyst. With ferrocenedicarboxylic acid (**5**) the oxidized electron mediator is attracted by the protonated merocyanine isomer state, and **3b**-GOx acts as the switched "on" biocatalyst. The neutral nitrospiropyran unit in **3a**-GOx lacks electrical attractive interactions for oxidized **5** and hence this state of the biocatalyst represents the switched "off" protein. With 1-[1-(dimethylamino)ethyl]ferrocene (**6**), the positively charged electron mediator is electrostatically repelled by the protonated merocyanine and **3b**-GOx is the switched-off state of the enzyme. Upon photoisomerization to **3a**-GOx, the electrical repulsion of oxidized **6** is eliminated and electrical communication with the FAD redox site is facilitated. This activates the enzyme in **3a**-GOx state for the bioelectrocatalyzed oxidation of glucose, switch "on".

We now compare the effectiveness of electrical communication of the $FADH_2$ center and the electrode surface by ferrocenecarboxylic acid (**4**) and ferrocenedicarboxylic acid (**5**). The oxidized state of **4** is overall neutral, while for oxidized **5** it is negatively charged. For both electron mediators, the reconstituted enzyme state **3b**-GOx is the switched-on biocatalyst and the enzyme form **3a**-GOx represents the deactivated switched-off protein. Note, however, that for ferrocenecarboxylic acid (**4**), the Michaelis−Menten analysis revealed only

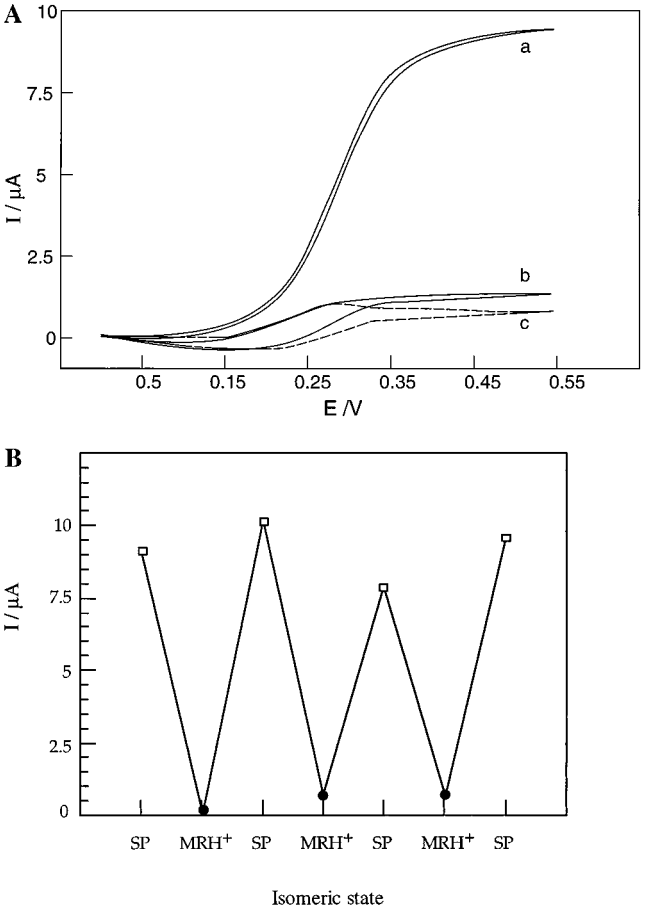

Figure 11. (A) Cyclic voltammograms for the bioelectrocatalyzed oxidation of glucose, 50 mM, and **6**, 0.15 mM, in the presence of (a) (SP-FAD)-GOx, 0.46 mg mL^{-1}; (b) (MRH^+-FAD)-GOx, 0.46 mg mL^{-1}; and (c) no enzyme. All experiments were recorded under the same conditions as described in Figure 4. (B) Cyclic amperometric transduction of optical signals recorded by the reconstituted photoisomerizable GOx, 0.46 mg mL^{-1}, **6**, 0.15 mM, and glucose, 50 mM, present in the electrolyte solution. Net electrocatalytic currents at $E =$ 0.4 V are presented.

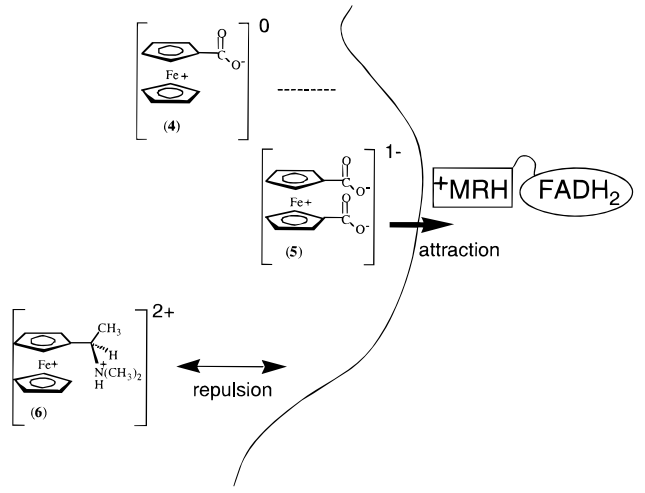

Figure 12. Schematic illustration representing the influence of the charge on the ferrocenium ions and its distance from the positively charged MRH^+-$FADH_2$ redox center.

a moderate difference in the K_m values, while the similar analysis for **5** reveals a significant difference in the respective K_m values of the electron mediator cosubstrate to the enzyme states **3a**-GOx and **3b**-GOx. With ferrocenedicarboxylic acid (**5**) the similar photochemical switch direction as for **4** is obtained. The Michaelis−Menten analysis of the enzyme activities of the two photoisomer states, **3a**-GOx and **3b**-GOx in the presence of **5**, reveals, however, a large difference of the respective K_m values. In fact, a substantial difference in the bioelectrocatalytic anodic currents originating from the **3a**-GOx and **3b**-GOx states in the presence of glucose is observed within a broad concentration range of **5**. This indicates that **5** in its oxidized state exhibits a significantly higher affinity for penetration of the protein, as compared to **4**. This is attributed to the electrostatic attraction of oxidized **5** by the positively charged photoisomerizable unit in **3b**-GOx. This electrostatic attraction facilitates electrical communication between the electron mediator and the FAD unit. The electrostatic attractive interactions are missing in the system where ferrocenecarboxylic acid (**4**) is used as electron mediator. In this system only the structural steric effects induced by the photoisomerization influence the penetration paths of the electron relay.

A final point to consider relates to the origin of the enhanced electrocatalytic current observed in the presence of the negatively charged electron mediator **5** in the presence of **3a**-GOx, $I_{max} = 60\ \mu A$, as compared to the electrocatalytic saturation currents with oxidized **4** or **5** and the **3b**-GOx biocatalyst, $I_{max} = 9.6\ \mu A$ and $I_{max} = 60\ \mu A$, respectively. The saturation current is proportional to the electron-transfer rate from $FADH_2$ to the ferrocenyl electron mediator, under conditions where the enzyme is saturated with the electron relay. The redox potentials of the electron mediators **4**−**6** are almost identical, $E° \approx 0.2$ V. Hence, no difference in the electron-transfer driving force from $FADH_2$ to the respective ferrocenyl cations should have a significant contribution to the electrical contact efficiency. The experimental difference in the electron-transfer rates from the $FADH_2$ to the ferrocenyl cations, however, could be attributed to different distances prevailing in the protein assemblies between the diffusional electron mediator and the $FADH_2$ center. For each of the electron mediators we find similar I_{max} values in the presence of **3a**-GOx and **3b**-GOx. The I_{max} values are, however, different for the various electron mediators. The identical I_{max} values for each of the electron mediators in the presence of **3a**-GOx and **3b**-GOx imply similar electron-transfer distances, which are controlled by the protein channel. The high I_{max} observed with **5** in the presence of **3b**-GOx, $I_{max} = 60\ \mu A$, originates presumably from a short electron-transfer distance between the MRH^+-$FADH_2$ unit and the oxidized electron mediator controlled by attractive electrostatic interactions.

A further aspect relates to the stability of the reconstituted biocatalyst to act reversibly as photoswitchable biocatalyst. For ferrocenecarboxylic acid (**4**) as electron-transfer mediator, we cycled to "on"−"off" photostimulated bioelectrocatalytic function of the enzymes for 15 cycles without a noticeable degradation of the biocatalyst monolayer.

Conclusions

A novel approach to assemble photoswitchable enzymes by protein reconstitution with a photoisomerizable FAD cofactor is demonstrated. We specifically addressed the transformation of the flavoenzyme glucose oxidase to an "on−off" photostimulated system by the reconstitution of apo-glucose oxidase with a synthetic photoisomerizable FAD analog. The resulting semisynthetic photoisomerizable flavoenzyme states **3a**-GOx and **3b**-GOx exhibit light-stimulated bioelectrocatalytic activities. The photochemically controlled bioelectrocatalytic features of the enzyme photoisomer states provide a means for the amperometric transduction of optical signals recorded by the enzyme−monolayer electrode. As the optical signal triggers

"on" a biocatalytic transformation, the optical information translates into a catalytic anodic current or an amplified amperometric response. Thus, the photoswitchable enzyme−monolayer electrodes represent active interfaces for the amplified amperometric transduction of recorded optical signals. These functionalized biocatalytic electrodes could be applied in the future as active materials for information storage and processing (biological computers), for the amplification of weak light signals, and for use as biological actinometers.

The detailed kinetic analyses of the bioelectrocatalyzed oxidation of glucose by the photoisomer states **3a**-GOx and **3b**-GOx in the presence of a series of electron mediators allowed us to elucidate the origin of the photoswitchable bioelectrocatalytic properties of the photoisomerizable enzyme: The photoisomerizable unit linked to the FAD redox center controls the penetration path of the electron-transfer mediator to the FAD site. Control of the penetration path is accomplished by two complementary mechanisms; steric structural perturbations of the penetration pathway and electrostatic attraction or repulsion of the electron mediator along the penetration route.

In addition to the fundamental understanding of the mechanisms controlling the bioelectrocatalytic activities of reconstituted photoisomerizable glucose oxidase in the presence of different electron mediators, the importance of the results rest in the ability to control and pre-design the "on−off" switch direction. That is, by the application of **5** as electron mediator, **3b**-GOx is the bioelectrocatalytic active enzyme where with **6**, **3a**-GOx is the photochemically switched-on biocatalyst.

Reconstitution of apo-glucose oxidase with the semisynthetic photoisomerizable FAD cofactor **3**, represents a unique example of a photoisomerizable switchable enzyme with a site-specific positioning of the photoactive unit in the protein. The available X-ray structure of glucose oxidase[22] suggests that computational assessment of the structural effects of the photoisomerizable units on the protein configuration is feasible. The photoswitchable properties of the reconstituted enzymes and the amplified amperometric transduction of the recorded optical signal by the electrobiocatalyzed transformation reveal new means to apply proteins in optobioelectronic devices.

Acknowledgment. This research was supported by the Israel Ministry of Science and Technology and the Bundesministerium für Bildung und Forschung (BMBF), Germany.

JA972663V

(22) Hecht, H. J.; Kadisz, H. M.; Hendle, J.; Schmid, R. D.; Schomburg, D. *J. Mol. Biol.* **1993**, *229*, 153.